Ministry of Science and Higher Education
Republic of Poland

JAGIELLONIAN UNIVERSITY IN KRAKÓW

EUROPEAN SPACE AGENCY

FRINGE 2026

15 - 19 June 2026 | Auditorium Maximum of the Jagiellonian University, Kraków, Poland

Exploiting Zero Baseline Interferometric Coherence for Biomass Retrieval

Wenyu Yang[1] Hossein Aghababaei[2]
[1]University of Napoli Parthenope, Italy
[2]University of Twente, The Netherlands

June 15, 2026

BACKGROUND

Above Ground Biomass (AGB): dry organic matter in stems, bark, and branches per unit area.

- Key variable for climate-system change and carbon-cycle analysis.
- Supports forest management, emissions reduction, and sustainable-development policy.

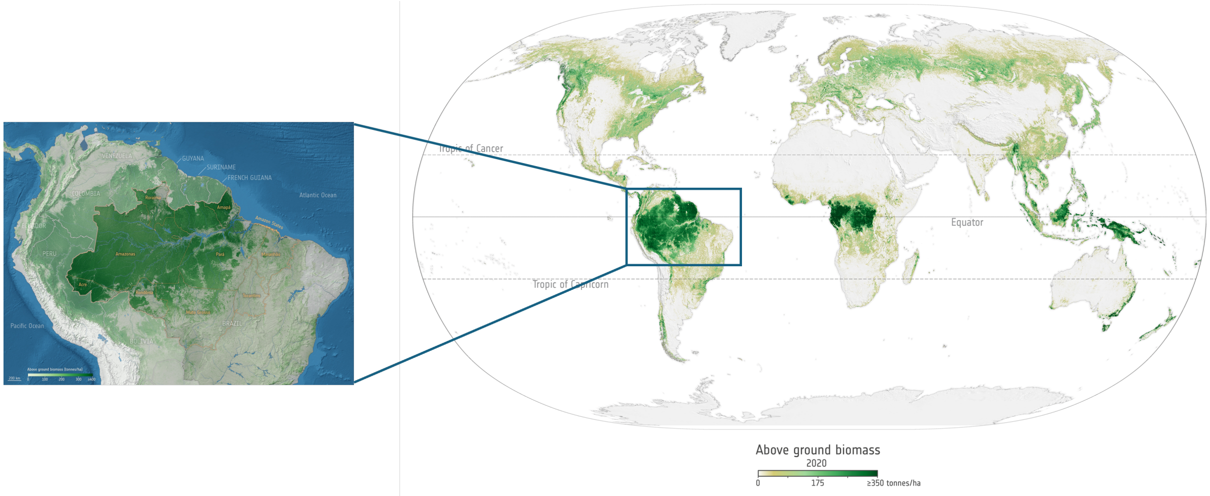

Figure. Global Above Ground Biomass 2022. Figure source: European Space Agency (ESA).

Approaches for AGB mapping

Optical and LiDAR approaches

- Inventory + allometry: accurate plots, but wall-to-wall maps need extrapolation.
- Optical mapping: useful indices and texture, but limited by cloud cover and saturation.
- LiDAR: strong height/structure constraints, but limited or sparse coverage.

SAR frequency bands

- C-band: time-series sensitivity, but shallow penetration and early saturation.
- L-band: better sensitivity to woody components; HV often outperforms HH.
- P-band: strongest penetration and sensitivity in dense forests.
- Multi-frequency fusion: combines surface, volume, terrain, and moisture information.

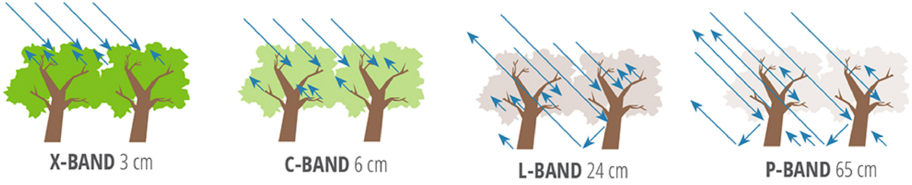

Figure. SAR wavelength controls penetration depth and dominant scattering layer. Figure source: NASA.

Backscatter-based approaches

- Empirical regression models: simple, but often miss the full backscatter–biomass relationship.

$$\sigma^0_{\mathrm{for}} = a + b\left(1 - exp\left(-\beta B\right)\right). \tag{1}$$

- Semi-empirical and physical models: represent key scattering mechanisms with few terms, e.g., the Water Cloud Model.

$$\sigma^0_{\mathrm{for}} = \sigma^0_{\mathrm{gr}} \exp(-\beta B) + \sigma^0_{\mathrm{veg}} \left[1 - \exp(-\beta B)\right] \tag{2}$$

- Non-parametric models: ingest many predictors, but often black-box machine-learning models.

Coherence-based approaches

- Empirical regression models: simple, but omit volume-decorrelation physics.
- Semi-empirical and physical models: e.g., the Interferometric Water Cloud Model (IWCM).

Backscatter is modeled as:

$$\sigma^0_{\text{for}} = \sigma^0_{\text{gr}} T_{\text{for}} + \sigma^0_{\text{veg}} (1 - T_{\text{for}}) . \qquad (3)$$

- σ^0_{gr}: ground contribution.
- σ^0_{veg}: vegetation contribution.
- T_{for}: two-way transmissivity, parameterized as $T_{\text{for}} = \exp(-\beta B)$.

$$\sigma^0_{\text{for}} = \sigma^0_{\text{gr}} \exp(-\beta B) + \sigma^0_{\text{veg}} [1 - \exp(-\beta B)] \qquad (4)$$

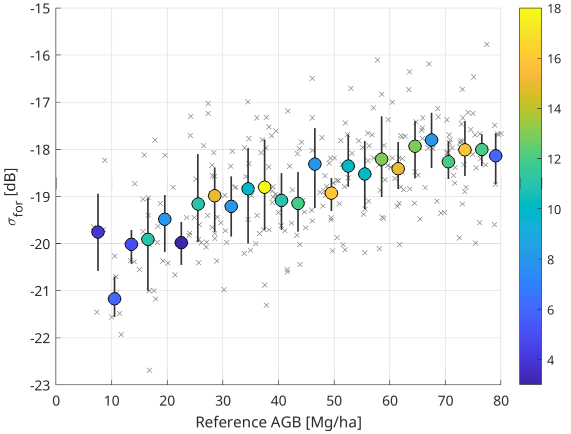

Figure. The SAR backscatter increases from a bare surface to the densest forest.

Key point

SAR backscatter sensitivity depends on sensor wavelength/polarization, forest type, phenology, terrain, and moisture.

COHERENCE-BASED MODEL

C-band backscatter saturates at relatively low AGB. Coherence may preserve sensitivity at higher biomass.

For two coregistered SLC acquisitions $s(t_1)$ and $s(t_2)$, the interferometric coherence is:

$$\gamma(t_1, t_2) = \frac{E\{s(t_1)s(t_2)^*\}}{\sqrt{E\{|s(t_1)|^2\}E\{|s(t_2)|^2\}}}. \tag{5}$$

It is affected by surface/volume decorrelation, temporal decorrelation, and thermal noise.

The Interferometric Water Cloud Model (IWCM) describes forest coherence as ground and canopy contributions Santoro et al., 2002:

$$\gamma_{\text{for}} = \gamma_{\text{gr}} \frac{\sigma^0_{\text{gr}}}{\sigma^0_{\text{for}}} \exp(-\beta B) + \frac{1-\exp(-\beta B)}{1-T_{\text{tree}}} \gamma_{\text{veg}} \frac{\sigma^0_{\text{veg}}}{\sigma^0_{\text{for}}} \frac{\alpha}{\alpha - j\frac{4\pi B_n}{\lambda R \sin\theta}} \left[\exp\left(-j\frac{4\pi B_n}{\lambda R \sin\theta} h\right) - T_{\text{tree}}\right]. \quad (6)$$

- γ^0_{gr}, γ^0_{veg}: ground and vegetation coherence.
- Volume decorrelation is induced by spatial baseline B_n.

For Sentinel-1, small effective baselines make $k_z \approx 0$.

$$B_n = 0, \quad (7)$$

$$\gamma_{\text{for}} = \gamma_{\text{gr}} \frac{\sigma^0_{\text{gr}}}{\sigma^0_{\text{for}}} e^{-\beta B} + \gamma_{\text{veg}} \frac{\sigma^0_{\text{veg}}}{\sigma^0_{\text{for}}} \left(1 - e^{-\beta B}\right) \quad (8)$$

Coherence Optimization

Eq.(8) has many unknowns, making inversion ill posed. With dual-pol data, polarization optimization identifies channels that maximize vegetation-decorrelation sensitivity De Petris et al., 2025.

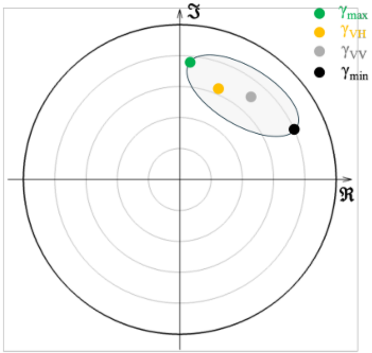

Figure. Interferometric coherence loci for dual-polarimetric data

- γ_{max}: vegetation-dominated coherence;
- γ_{min}: coherence retaining ground scattering.

IWCM becomes:

$$|\gamma_{\mathrm{min}}| = \left| \gamma_{\mathrm{gr}} \frac{\sigma^0_{\mathrm{gr},1}}{\sigma^0_{\mathrm{for},1}} e^{-\beta_1 B} + \gamma_{\mathrm{veg,min}} \frac{\sigma^0_{\mathrm{veg},1}}{\sigma^0_{\mathrm{for},1}} \left(1 - e^{-\beta_1 B}\right) \right| \tag{9}$$

$$|\gamma_{\mathrm{max}}| = \left| \gamma_{\mathrm{veg,max}} \frac{\sigma^0_{\mathrm{veg},2}}{\sigma^0_{\mathrm{for},2}} \left(1 - e^{-\beta_2 B}\right) \right| \tag{10}$$

Combining coefficient:

$$\begin{aligned} \text{Ground–Forest model:} \quad & |\gamma_{\mathrm{min}}| = \left| a_{\mathrm{min}} e^{-\beta_1 B} + b_{\mathrm{min}} \left(1 - e^{-\beta_1 B}\right) \right|, \\ \text{Only–Ground model:} \quad & |\gamma_{\mathrm{min}}| = \left| a_{\mathrm{min}} e^{-\beta_1 B} \right|, \\ \text{Only–Forest model:} \quad & |\gamma_{\mathrm{max}}| = \left| a_{\mathrm{max}} \left(1 - e^{-\beta_2 B}\right) \right|. \end{aligned} \tag{11}$$

Study area and dataset

Sentinel-1 and NISAR SAR data over Kotka, Finland were used.

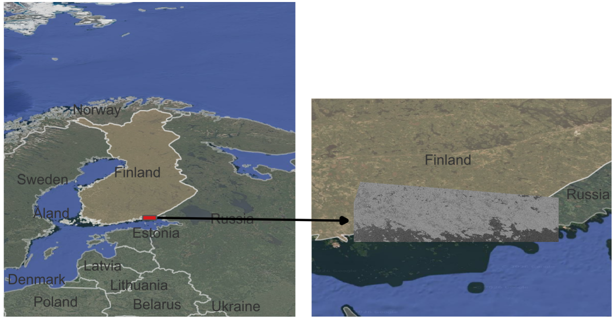

Figure. Study area at Kotka, Finland

Table. List of datasets.

Dataset	**Variable**	**Data dates**
Sentinel-1 GRD	backscatter σ^0	07 Jun. - 05 Oct. 2021
Sentinel-1 InSAR pair	Coherence γ^0	05 Nov. 2025 - 17 Jan. 2026
NISAR InSAR pair	Coherence γ^0	01 Nov. 2025 - 12 Jan. 2026
Forest inventory plots	AGB	2021
LiDAR	Canopy height	2021

AGB MAP FROM FOREST HEIGHT

Santoro et al., 2022 expresses AGB as a function of forest height h.

$$B = p_1 h^{p_2} \tag{12}$$

Plot inventory calibration gave $p_1 = 2.2$ and $p_2 = 1.5$.

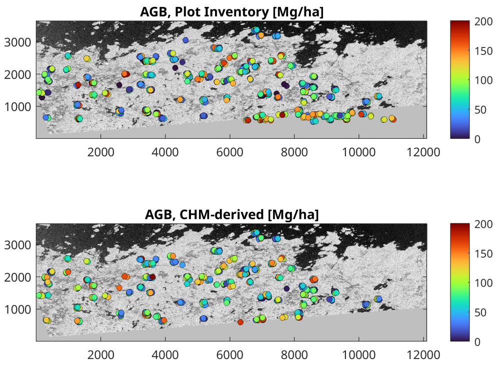

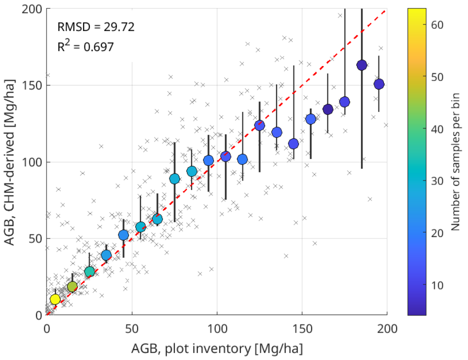

Interpretation

When AGB is below 130 Mg/ha, CHM-derived AGB aligns well with plot inventory.

Fitting strategy

Models were fitted on grid-cell averages of SAR observables and reference AGB.

- Tested cell sizes: 100–500 m.
- Fixed β during each fit; swept $\beta = 0.02$–0.10.
- Used least-squares minimization for each setting.
- Evaluated RMSD and agreement with reference AGB.

$$\hat{\Theta} = \arg\min_{\Theta} \sum_{i=1}^{N} \left(y_i - \hat{y}_i(\Theta, B_i)\right)^2 \tag{13}$$

- y_i: measured SAR observable.
- $\hat{y}_i$: modelled observable.
- Θ: fitted model parameters.

Backscatter model fitting

WCM model for VH and VV backscatter:

$$\sigma^0_{\mathrm{for}} = \sigma^0_{\mathrm{gr}} \exp(-\beta B) + \sigma^0_{\mathrm{veg}} \left[1 - \exp(-\beta B)\right] \quad (14)$$

For each polarization and fixed β, σ^0_{gr} and σ^0_{veg} are estimated by:

$$\sum_{i=1}^{N} \left[\sigma^0_{\mathrm{meas},i} - \sigma^0_{\mathrm{model},i}\left(\sigma^0_{\mathrm{gr}}, \sigma^0_{\mathrm{veg}}, B_i\right)\right]^2 = min \quad (15)$$

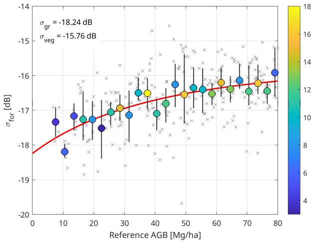

VH backscatter vs reference AGB

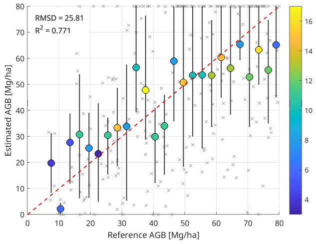

Estimated AGB vs reference AGB

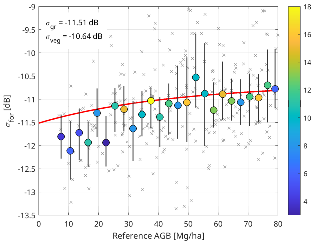

VV backscatter vs reference AGB

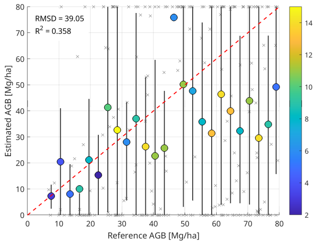

Estimated AGB vs reference AGB

Ministry of Science and Higher Education Republic of Poland

Jagiellonian University in Kraków

European Space Agency

Backscatter-based AGB estimation

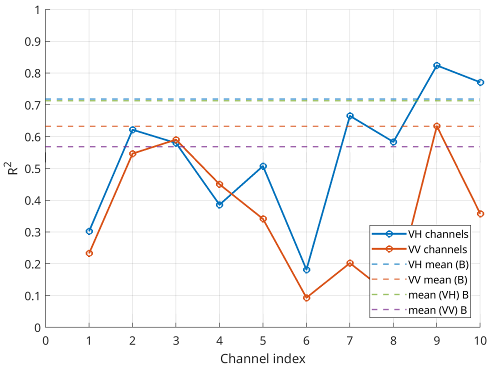

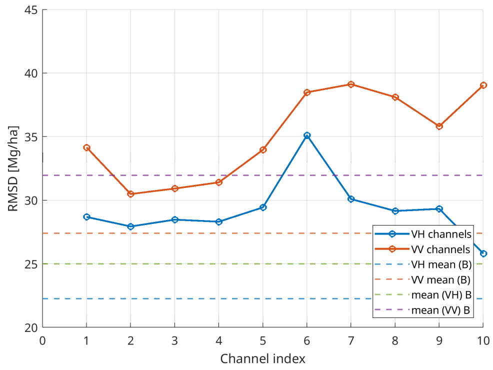

Result

- VH estimates agree better with reference AGB than VV.
- Multi-channel combinations improve performance.
- Backscatter inversion still saturates at high biomass.

PERFORMANCE WITH β AND CELL SIZE

Performance was evaluated for $\beta = 0.02$–0.10 and 100–500 m cells.

- At 100 m, performance is stable for $\beta > 0.04$.
- At 300 m, performance decreases as β increases.
- Larger cells generally reduce performance.

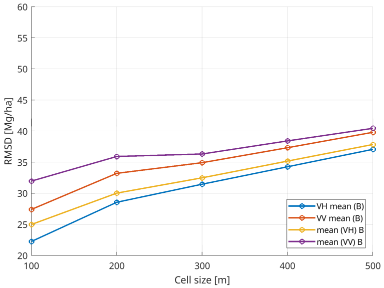

$\beta = 0.02$

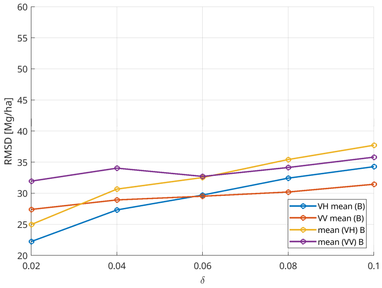

Cell size: 100 m $\times$ 100 m

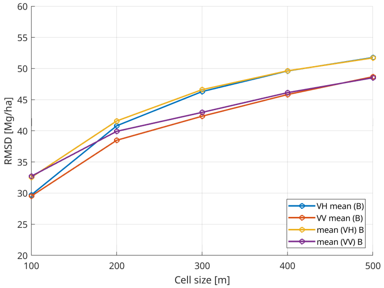

$\beta = 0.06$

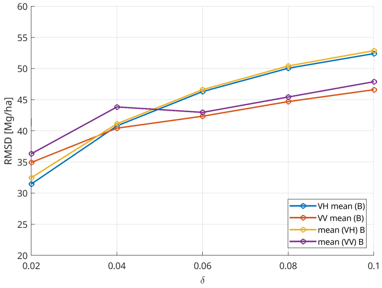

Cell size: 300 m $\times$ 300 m

$\gamma_{\max}$ MODEL FITTING

$\gamma_{\max}$ is treated as vegetation dominated. Its zero-baseline coherence with AGB relation is:

$$|\gamma_{\max}| = \left|a_{\max}\left(1 - e^{-\beta_2 B}\right)\right| \tag{16}$$

For fixed β_2, $a_{\max} \in [0, 1]$ is estimated by:

$$\sum_{i=1}^{N} \left[\gamma_{\text{meas,max},i} - \gamma_{\text{model},i}\left(a_{\max}, \beta_2, B_i\right)\right]^2 = min. \tag{17}$$

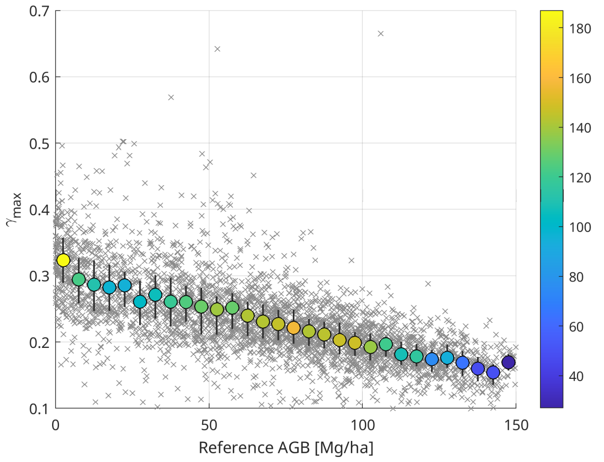

C-band $\gamma_{\max}$ vs AGB

γ_{max}-BASED AGB ESTIMATION

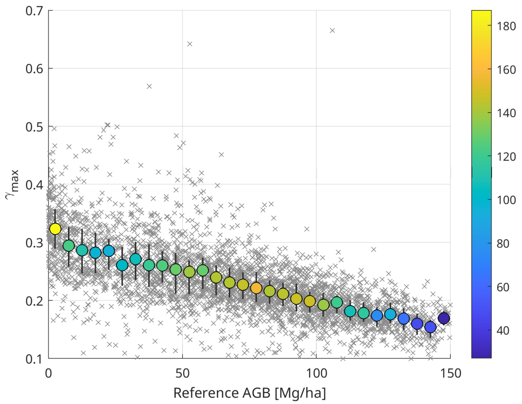

γ_{max} vs reference AGB

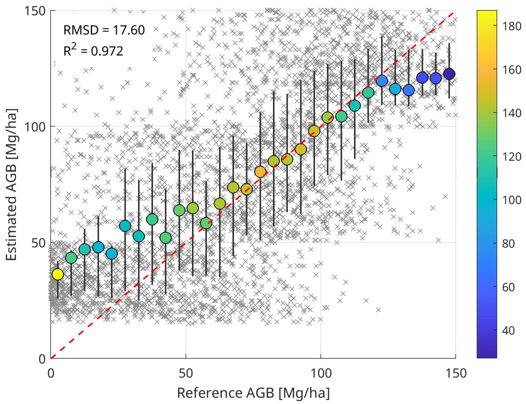

Estimated AGB vs reference AGB

Observation

- C-band γ_{max} gives clear relationship with AGB.
- Estimated AGB has good agreement with AGB reference.

Performance was evaluated for $\beta = 0.02$–0.10 and 100–500 m cells.

- Performance is weakly sensitive to β.
- Larger cells generally improve performance.

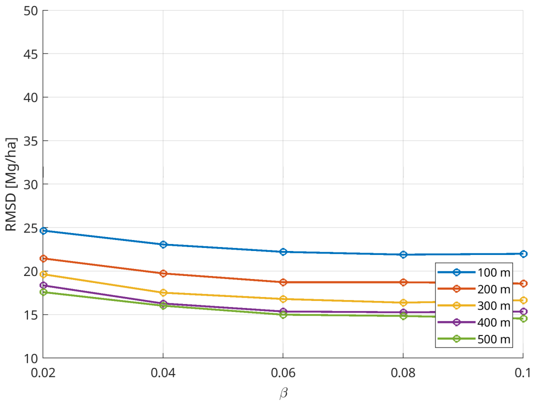

C-band: cell size 500 m $\times$ 500 m

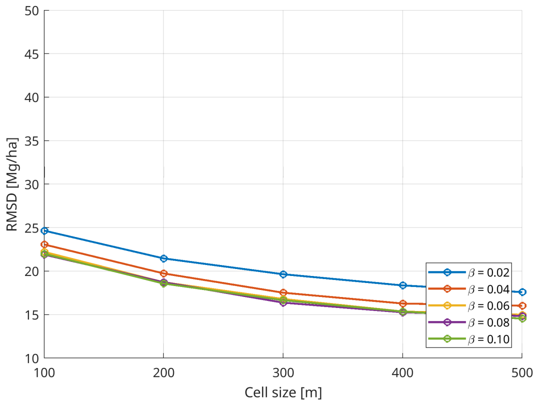

C-band: $\beta = 0.02$

γ_{min} retains stronger ground contribution. Two formulations were tested.

Ground–Forest model

$$|\gamma_{\mathrm{min}}| = \left|a_{\mathrm{min}} e^{-\beta_1 B} + b_{\mathrm{min}} \left(1 - e^{-\beta_1 B}\right)\right| . \tag{18}$$

Only–Ground model

$$|\gamma_{\mathrm{min}}| = \left|a_{\mathrm{min}} e^{-\beta_1 B}\right| . \tag{19}$$

Fitted coefficients were constrained to $[0, 1]$.

$$\sum_{i=1}^{N} \left[\gamma_{\mathrm{meas,min},i} - \gamma_{\mathrm{model},i}\left(\Theta, \beta_1, B_i\right)\right]^2 = min \tag{20}$$

Purpose

The comparison tests whether the vegetation term improves inversion or mainly adds degrees of freedom.

γ_{min}-based AGB estimation: Ground–Forest model

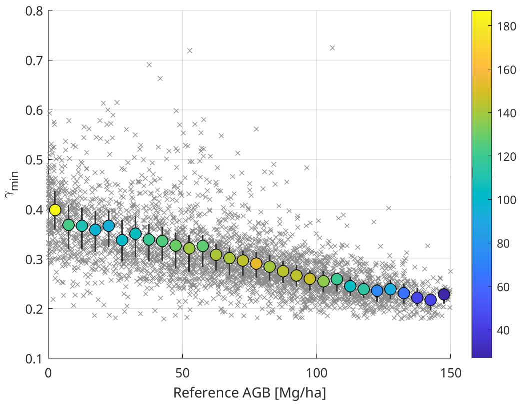

γ_{min} vs reference AGB

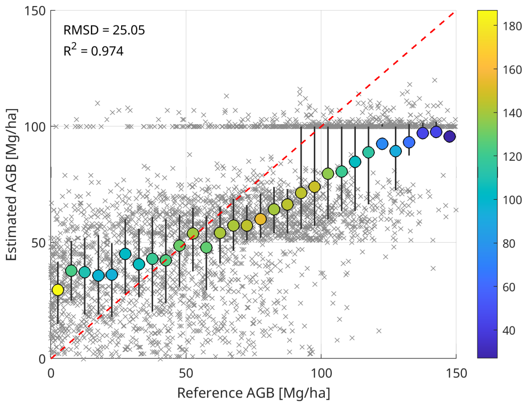

Estimated AGB vs reference AGB

Observation

- C-band γ_{min} gives clear relationship with AGB.
- Estimated AGB has good agreement with AGB reference.

$\gamma_{\min}$ FITTING SENSITIVITY: GROUND–FOREST MODEL

Performance was evaluated for $\beta = 0.02$–0.10 and 100–500 m cells.

- C-band is weakly sensitive to β and cell size.

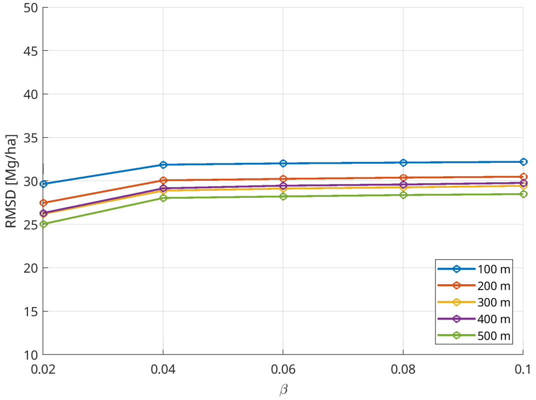

C-band: cell size 500 m × 500 m

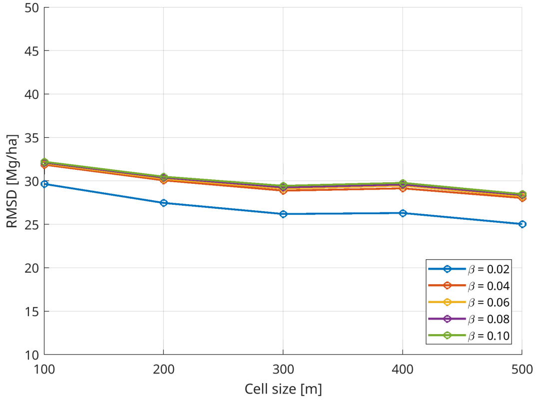

C-band: β = 0.02

γ_{min}-BASED AGB ESTIMATION: GROUND–FOREST MODEL VS ONLY–GROUND MODEL

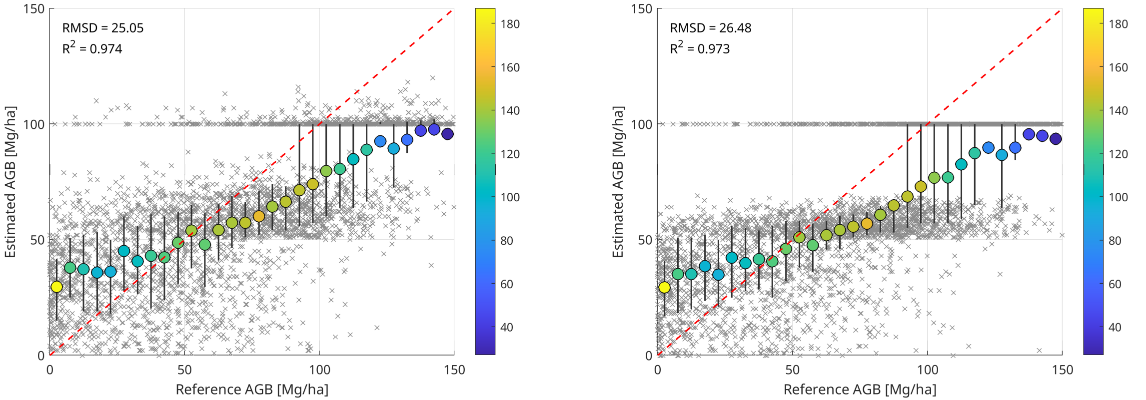

Ground–Forest Model Only–Ground Moel

Observation

- Only–Ground Model performs slightly worse than the Forest–Ground Model.

Experiment

L-band coherence-based model preliminary results

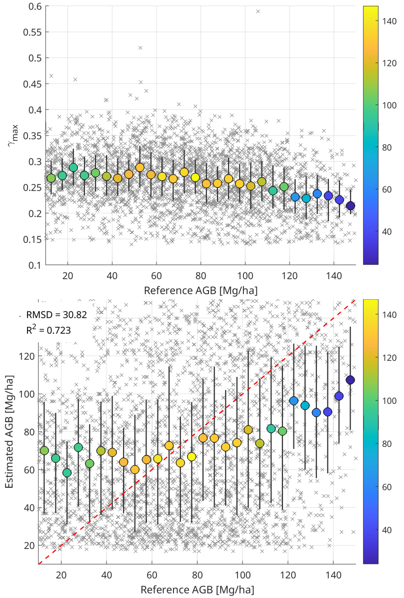

γ_{max}: Only–Forest model

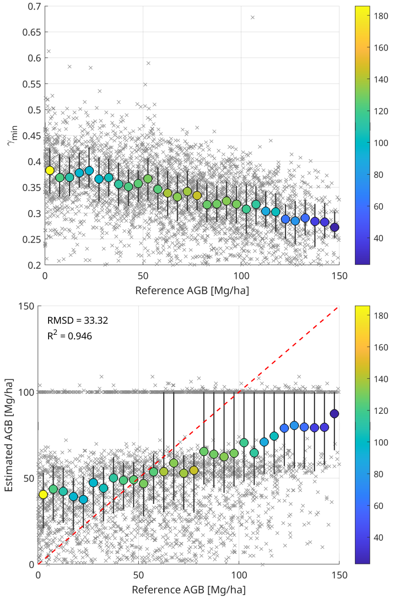

γ_{min}: Ground–Forest model

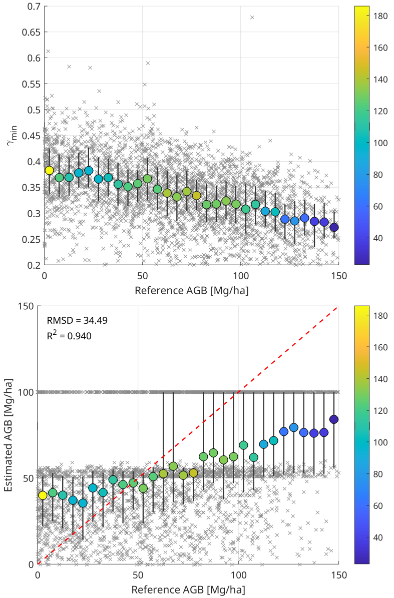

γ_{min}: Only–Ground model

- Backscatter-based Model:
  - VH estimates AGB better than VV.
  - C-band captures part of the AGB signal, but saturates in denser forest ($>$ 80 Mg/ha).
  - Time-series combinations improve retrieval performance.
- Coherence-based Model: optimized zero-baseline coherence adds a biomass-sensitive observable.
  - γ_{max}: vegetation-dominated channel; C-band performs best, with RMSD around 15–25.
  - γ_{min}: retains ground information, but performs worse than γ_{max}.

Remaining limitations

- Reference-map errors propagate into fitting.
- Optimized coherence still depends on temporal decorrelation, noise, and registration errors.

References

- De Petris, S., Pardini, M., Borgogno-Mondino, E., Prats, P., & Papathanassiou, K. (2025). **An evaluation of the pol-insar forest height estimation performance with dual polarimetric insar data [Presentation 1217].** *Proceedings of the Living Planet Symposium 2025*, 1–6.
- Santoro, M., Askne, J., Smith, G., & Fransson, J. E. (2002). **Stem volume retrieval in boreal forests from ERS-1/2 interferometry.** *Remote Sensing of Environment*, *81*(1), 19–35. https://doi.org/10.1016/S0034-4257(01)00329-7
- Santoro, M., Cartus, O., Wegmüller, U., Besnard, S., Carvalhais, N., Araza, A., Herold, M., Liang, J., Cavlovic, J., & Engdahl, M. E. (2022). **Global estimation of above-ground biomass from spaceborne C-band scatterometer observations aided by LiDAR metrics of vegetation structure.** *Remote Sensing of Environment*, *279*, 113114. https://doi.org/10.1016/j.rse.2022.113114